OSIRIS Large Guaranteed Time Programs

J. Cepa[1,2], A. Bongiovanni[1], M. Ramón–Pérez[1] A.M. Pérez García[3], E.J. Alfaro[4], H.O. Castañeda[5], M. Cerviño[1,4], J. Gallego[6], J.J. González[7], J.I. González–Serrano[8], M.A. Lara–López[7], R. Pérez–Martínez[3], I. Pintos–Castro[3], M. Sánchez–Portal[9], J. Bland-Hawthorn[10], and D.H. Jones[11]

[1] Instituto de Astrofísica de Canarias, E–38200 La Laguna, Tenerife, Spain
[2] Departamento de Astrofísica, Universidad de La Laguna, E-38206 La Laguna, Tenerife, Spain
[3] Herschel Science Centre, ESAC/INSA, P.O. Box 78, 28691 Villanueva de la Cañada, Madrid
[4] Instituto de Astrofísica de Andalucía (CSIC), Apdo. 3004, E–18080, Granada, Spain
[5] Departamento de Física, Escuela Superior de Física y Matemática, IPN, México D.F., Mexico
[6] Departamento de Astrofísica y CC de la atmósfera, Universidad Complutense de Madrid, 28040 Madrid, Spain
[7] Instituto de Astronomía, Universidad Nacional Autónoma de México, Apdo Postal 70-264, Cd. Universitaria, 04510, Mexico
[8] Instituto de Física de Cantabria, CSIC-Universidad de Cantabria, Santander, Spain
[9] European Southern Observatory, Alonso de Córdova 3107, Vitacura 19001, Santiago de Chile, Chile
[10] Sydney Institute for Astronomy, School of Physics A28, University of Sydney, NSW 2006, Australia
[11] School of Physics and Astronomy, Monash University, Victoria 3800, Australia

Abstract

The status of OTELO and Lockman SpReSO surveys, the two large guaranteed time programs currently under way using OSIRIS at the 10.4m GTC is presented. The OTELO project, designed to detect the main optical emission lines from Hα to Lyα at redshifts from 0.4 through 7, is the deepest emission line survey to date, with unprecedented sensitivity in the detection of small equivalent widths. Lockman SpReSO is aimed to obtaining optical spectra, up to 24.5 AB magnitudes, in the central 24×24 square arcminutes of the Lockman Hole field, which has been observed with ROSAT and XMM–Newton at the highest depth. Lockman SpReSO mainly targets Far Infrared sources detected with the Herschel Space Observatory.

1 Introduction

Deep multi–wavelength extragalactic surveys have become an essential tool for studying galaxy formation and evolution, providing basic information about cosmological parameters, and even setting stringent limits on neutrino species and masses. While extragalactic broad band imaging and most spectroscopic surveys select targets based on their continuum, selection through emission lines via narrow–band imaging (see [42] and references therein) provides a complementary view.

Within narrow–band surveys, those using tunable filters (TF) as the OSIRIS Tunable Emission Line Object survey (OTELO [6]), CADIS (Calar Alto Deep Imaging Survey [43]), and the TTFFGS (Taurus Tunable Filter Faint Galaxy Survey [17]) detect one order of magnitude more objects (normalizing for telescope size and exposure time) than conventional narrow band surveys as those using Suprime–Cam at Subaru [16]. Then, narrow band surveys with Tunable Filters in large telescopes constitute a deep sky probe with unprecedented sensitivity. Moreover, since tunable filter surveys obtain a set of images of the same pointing at slightly different wavelengths, this technique can be rather considered low resolution 3D wide field spectroscopy than conventional narrow–band imaging.

For these reasons, the TFs of OSIRIS provide GTC with unique capabilities compared with similar sized telescopes, and the higher depth of OTELO supplies a unique database in sensitivity, and spectral resolution. More detailed information about the data reduction, the survey and its demographics can be found in [4].

Within spectroscopic surveys, and in spite of the apparent wealth of data, gathering statistically significant samples of faint galaxies (i.e. $\geq$24.5 AB magnitudes) in different, sub–horizon scale areas of the sky, overcoming (and characterizing) cosmic variance, is still an issue. Lockman Spectroscopic Redshift Survey using OSIRIS (Lockman SpReSO) will constitute one of the deepest spectroscopic surveys ever made: compared with other deep or ultra-deep spectroscopic surveys, Lockman SpReSO will reach a depth parameter [12] a factor 1.2 larger than the on-going VVDS/ultra–deep survey [24]. Furthermore, this survey is more advantageous than z-COSMOS and AEGIS–DEEP regarding the sensitivity at the continuum and the spectral coverage, respectively.

2 OTELO

2.1 Observations

OTELO [6] is aimed at surveying emission line objects using OSIRIS tunable filters in a selected atmospheric window relatively free of sky emission lines between 907–928 nm. This aim has been fulfilled by investing 108 dark hours of guaranteed observing time in a single OSIRIS pointing at the Extended Groth Strip (EGS). The wavelength range has been covered by observing 36 contiguous wavelengths with a FWHM of 1.2nm, scanning every 0.6nm (i.e.: half the FWHM), equivalent to a spectral resolution of ∼700 (Table 1). This sampling allows efficiently deblending Hα from [NII]λ6583Å [26]. Each wavelength has been observed during 6600 seconds distributed in 6 exposures of 1100 seconds dithered 18 arcseconds in a cross–

shaped pattern to fill out the gap between detectors, and to identify diametric ghost images. The guaranteed time invested came from the OSIRIS instrument team and the IAC.

The final observations were obtained in June 2014 and the data are already fully reduced and calibrated, the sources extracted, and the resulting catalogue correlated with ancillary data from X–Ray through cm. The mean seeing during the observations was of 0.8 arcsec, as measured directly on the scientific images. The best seeing corresponds to 0.64 arcsec. The TF tuning during the observations was found stable at the nominal accuracy of 0.1nm, as expected.

2.2   Data reduction hints

Most of the data reduction process was performed using standard IRAF routines. Bias was first subtracted, and the images were trimmed. Cosmic rays were removed, and flatfielding was achieved by fitting a 2D surface to the data, since sky flats were not available, and dome flats are not useful due to differential illumination effects. Illumination was also corrected, and airglow was subtracted. Sky rings were subtracted by 2D fitting of a surface symmetric with respect to the optical centre of the TF, after iteratively masking objects at 3σ level. A median combination of dithered images provide a fringe map that was subtracted to the data, providing fringe corrected images.

For each image, astrometry was performed using stars of $z' <23.0$ magnitudes of the Canada–France–Hawaii Telescope Legacy Survey (CFHTLS), and the matched images of the same wavelength combined (Fig. 1 left). Finally the sources were extracted with SExtractor [3] in dual mode using the deep image (hereafter OTELONB) resulting from coadding selected images of each slice by using a clipping algorithm, synthesizing a filter centered at $\sim$914 nm and 21 nm wide at the optical centre. Then, the centre to edge wavelength variation was corrected based on the TF optical centre, and the new wavelength dependence derived by the OSIRIS instrument team [19]. Finally, flux calibration was achieved using two standard spectrophotometric stars within the same field, via PSF fitting photometry, yielding a photometric accuracy of ±0.05 magnitudes at a S/N>3. The photometry allows deriving plots of flux vs. wavelength for each source usually termed pseudo–spectra (Fig. 1 right), since their properties are different from that of standard spectra, even if they resemble them.

A total of more than 11237 raw sources were extracted from the deep image OTELONB, with a minimum detectable flux of 2×10^{-20} erg/cm^2/s/AA (3σ, 50% completeness, Fig. 2), equivalent to 26.53 AB magnitudes, two magnitudes deeper than the deepest narrow band survey so far available. These figures are fully consistent with the OSIRIS ETC calculators provided by the OSIRIS instrument team and available in the GTC WWW.

Emission line objects were then detected using two techniques: via peaks in the pseudo–spectra (Fig. 1 right) and via colour–magnitude diagrams. The peaks in the pseudo–spectra were first detected using the authomated algorithm of [37] and confirmed after a careful visual examination of all pseudo–spectra. This procedure yield 1030 bona fide emitters in the OTELO wavelength range. For the colour–magnitude diagrams, the colour z–OTELONB were represented versus OTELONB, where z magnitude came from the CFHTLS, and OTELONB were the magnitudes from the OTELO deep image obtained adding selected
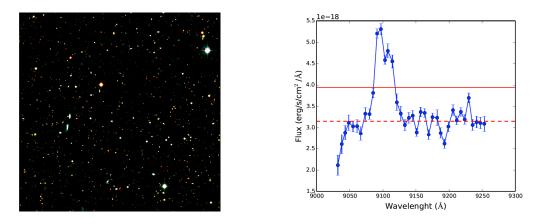
Figure 1: Left: Composite image of the OTELO field encompassing CFHTLS r & g bands plus OTELO deep image (OTELONB) obtained adding selected images together, as described in the text. North is at the top, East is at the left. Right: Pseudo–spectra of one z = 0.4 OTELO source showing the Hα plus [NII]λ6583Å emission lines. The dashed line is the continuum level and the solid line is 2σ above the continuum level.
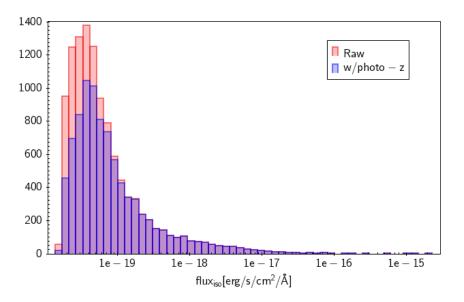

Figure 2: Histogram of the fluxes of the 11237 sources detected in OTELO survey. The minimum detectable flux at 3σ with 50% completeness is 2×10^{-20} erg/cm^2/s/AA, equivalent to 26.53 AB magnitudes, two magnitudes deeper than the deepest narrow band survey so far available. Light shadow corresponds to the whole sample of 11237 sources, while the darkest shadow represents the sample of more than 9000 sources with counterparts in the ancillary data.
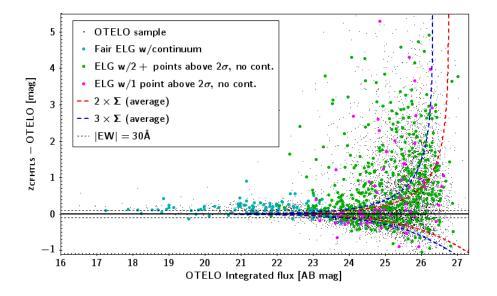
Figure 3:   A colour-magnitude diagram for emission line object selection. OTELO integrated flux (OTELONB in text) corresponds to the flux measured on the deep image of the survey. Colour is defined using the z-band from CFHTLS and the OTELONB data. Small black dots represent OTELO sources, and the large coloured ones are the bona-fide emitters (1031). Apart from the latter, additional 2253 sources show a colour $> 3 \times \Sigma$ limit (upper blue segmented curve), which constitutes a parallel set of emission line objects that are being also analysed. The dotted black lines represent arbitrary colour boundaries of $|EW| = 30$ Å.

images together, as described above. The emission line candidates can be detected as colour excess above a predefined Σ threshold. This procedure yields 2253 additional emission line candidates above 3Σ (Fig. 3).

2.3   Ancillary data

Data from OTELO survey is complemented with a multi–wavelength expression of each raw source. Reduced images from the Canada–France–Hawaii Telescope Legacy Survey (CFHTLS) in ugriz bands, F606W & F814W ones from the Advanced Camera for Surveys (ACS) of the Hubble Space Telescope (HST), and JHKs frames from WIRCAM Deep Survey (WIRDS), were carefully resampled and registered to the OTELO deep image OTELONB. Using SExtractor [3] in dual mode, we obtained PSF–fitting photometry for each raw source in these bands. The resulting catalog was correlated with selected data compilations of the All-Wavelength Extended Groth strip International Survey (AEGIS). This includes the photometric data in X-Ray from Chandra/ACIS-I 200 ks [33], NUV and FUV from the Galaxy Evolution Explorer (GALEX), although reprocessed and astrometrically matched to CFHT data by the authors, mid infrared from the Infrared Array Camera (IRAC), 24 μm from the Multiband Imaging Photometer (MIPS) [2], 100-500 μm from the Photodetector Array Camera and Spectrometer (PACS, [27]) and the Spectral and Photometric Imaging Receiver
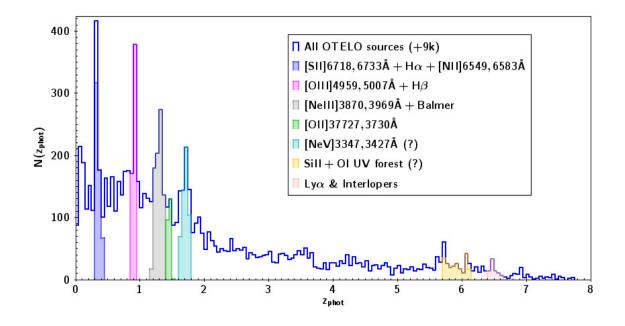
Figure 4: Preliminary photometric redshifts obtained for the more than 9000 OTELO sources with ancillary data counterparts.

(SPIRE, [31]), both onboard the Herschel Space Observatory, and VLA 6 & 20 cm. From the total 11237 raw sources of the catalogue, more than 9000 have counterparts in the ancillary data.

2.4 Photometric redshifts

The preliminary photometric redshifts, shown in Figure 4, were obtained using optical, NIR, MIR and FIR data from the ancillary data, including OTELONB photometry. Then, the data used for the photo–z encompassed broad band u' through 500 μm. The tool used for this purpose was LePhare ([1] and [22]) with a total of 14 templates: 4 representatives of Hubble types, 6 for starbursts (SBG), 1 representing quasar (QSO) and Active Galactic Nuclei (AGN), plus 3 for characterizing M, L, T stellar spectral types.

DEEP2 spectra (650–900 nm) up to z = 1.5 [30] were used for calibrating the photometric redshifts obtained. For the bona fide emitters, selected using the pseudo–spectra, the redshift accuracy is $|\Delta z/(1 + z)| < 0.1$ for 83% of the sample of emitters (Fig. 5), and for 79% of the total sample of sources.
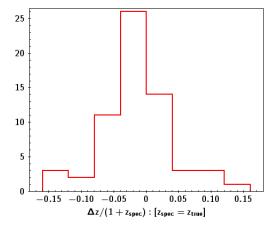
Figure 5:   Photometric redshift errors for the emitters selected via pseudo–spectra.

2.5   Science ongoing

There are several scientific programs currently ongoing and planned. The study of the fraction and properties of AGN/QSO at a redshift $\sim$0.4 involves deblending Hα from [NII]λ6583Å and using these emission lines for segregating AGN from SBG [7], in combination with X-Ray diagnostics from ancillary data, and also using N2 as metallicity estimator for SBGs [10]. More details can be found in [34].

Preliminary Stellar Masses for the sample of z=0.4 emitters will also provide a list of candidates to low–mass (dwarf) star–forming galaxies. The Spectral Energy Distribution (SED) of these objects will allow us to estimate their star formation history. To stablish if they formed most of their stars very early in the universe, or relatively late, is a very important evidence to determine the best overall galaxy evolution model. Finally, and because of the extreme depth of the OTELO survey, some dwarfs could also be identified at larger redshifts, and higher look–back times, setting additional constraints on galaxy evolution models.

The morphological classification of OTELO sources provides an essential parameter for characterizing the galaxy population, and studying trends versus morphology. To this aim, the high spatial resolution ACS/HST images are used applying GalSVM [21], and GALFIT [32]. The preliminary work has so far concentrated in galaxies brighter than 23rd magnitude [29].

The highest redshift component will allow providing constraints in the population of Lyman Alpha Emitters (LAEs) and Lyman Break Galaxies (LBGs), and studying their properties in follow–up observations [5].

2.6   Next steps

The next steps for obtaining the final catalogue are: consolidating the photometric redshifts, segregating the interloppers in the high redshift sample of LAEs and LBGs, extending the morphological analysis to the whole sample, and deriving methods for the morphological

Table 1: Main characteristics of OTELO Survey

Parameter	Value
Centre coordinates	α:14h17m20s, δ:+52°27'50''
Spatial coverage	49 arcmin^2
Wavelength coverage at the optical centre	9070 – 9280Å
FWHM	12Å
Sampling interval	6Å
Wavelength accuracy	1Å
Limiting magnitude (3σ, 50% completeness)	26.53 AB
Minimum EW	$\sim$3Å
Photometric accuracy S/N>3	$\pm$0.05 mag
Total sources extracted	11237
Bona fide emitters	1030
Candidate emitters	2253
Bona fide absorbers	147
Redshift accuracy	$\sim$5% up to z=1.4
Ancillary data	Deep X-Ray through 6 cm
ACS/HST	Yes
Deblending Hα from NII	Yes

classification of galaxies either too faint, or with a too small number of pixels, to apply the standard methods mentioned above.

The expected follow–up observations include spectroscopy in the optical using the Multiple Object Spectroscopy (MOS) of OSIRIS/GTC, and in the NIR using the MOS provided by EMIR/GTC. CO J:1→0 observations using the IRAM Plateau de Bure, and the Gran Telescopio Milimétrico (GTM) are also foreseen.

The next scientific objectives to be tackled are the detailed study of high redshift QSO/AGN, and the overdensities of Emission Line Galaxies (ELG).

3   Lockman SpReSO

3.1   Background

The Lockman Hole (hereafter LH) is the best reference among the most prominent extra-galactic fields regarding low Galactic hydrogen column density (NH=5.8×10^{19} cm^{-2}), [11]. For this reason the central part of this field has been targeted by e.g. ROSAT, XMM-Newton and GALEX missions, favouring it with very deep observations per solid angle unit. Moreover, this region of the LH has been observed at 100 and 160 μm in the framework of the PACS-Herschel Key Project of Guaranteed Time "PACS Evolutionary Probe" (PEP; [27]) with a depth of 6 mJy (at 5σ) over an area of $\sim$24×24 arcmin^2.

However, a surprising lack of deep optical spectroscopy in the LH is an unresolved issue despite the wealth of ancillary data (most recent compilation in [15]): in the whole LH field ($\sim$15 deg^2), there are barely $\sim$600 spectroscopic redshifts reported up to z=0.42, and only 115 X–Ray sources spectroscopically targeted ([38], [25], [44], [20]). Moreover, we have confirmed that e.g. from 786 optical counterparts (up to r=24.6 mag) of PEP/Herschel sources in the central LH field, only 40 have known spectroscopic redshifts (18 of these have available spectra), 16 of which correspond to bright (r < 20.7) sources.

3.2   Source selection

The main part of the sample comes from the 952 FIR sources detected with the Herschel Space Observatory. The FIR data have been already gathered, reduced, and the first catalogues extracted by the PEP Team. These observations allow sampling at or near the maximum of the SED of active star forming galaxies at high redshift (z=3), thus providing a good estimate of their bolometric luminosity, and with a good enough spatial resolution to establish a reliable cross-correlation with optical sources. Therefore, picking spectroscopic redshifts and derived parameters from emission/absorption lines features in the optical/NIR domain are mandatory to determine accurate luminosities, gas–phase metallicities, extinction corrected SFRs from standard indicators, as well as a robust spectral classification of these FIR sources with likely optical counterparts.

The total sample of 1171 targets includes also unestudied XMM sources, radio-galaxies [8], very red AGN (combining [18] and [35] criteria), SMG [28], and 185 Galactic targets (Table 2).

3.3   Observations

For covering the scientific objectives, 240 hours of guaranteed observing time will be invested in OSIRIS/GTC and EMIR/GTC MOS. The guaranteed time comes from the OSIRIS instrument team and the Instituto de Astronomía of the Universidad Nacional Autónoma de México (IA–UNAM).

At the time of writing this contribution, data for 30% of the total survey has already been collected, and their reduction is ongoing.

For a selected sample of high redshift sources, EMIR/GTC MOS using OSIRIS guaranteed time, will provide the optical emission lines redshifted to the NIR.

3.4   Scientific objectives

The first objective to be tackled is obtaining reliable redshifts via emission or absorption features, including D4000 and Lyman break. Emission lines will furnish optical/NIR SFR estimations via Balmer Hα luminosities [23], together with integrated attenuations using Hα/Hβ, and gas metallicities via R23 or N2 proxies [41], depending on the redshifted wavelength coverage and the line intensity. From these metallicity determinations and the FIR–based luminosities it would be possible to confirm the departures from the local L-Z relations

observed [36], and analysing possible dependences with LFIR and redshift, providing another clue for the chemical evolution of the FIR galaxies of our sample.

We aim also to further explore the difference among UV-corrected, optical and TIR derived SFRs (see a low-z approach in [13]), as well as the contribution of FIR galaxies to the evolution of the Star Formation Rate Density (SFRD) from z∼3, specially those related to the population of LAE, LBG, LIRG/ULIRG and SMG in different epochs. Finally, we expect gaining insight into the nature of FIR sources with different X–Ray properties derived from ancillary data, in addition to the optimal selection (e.g. [9]) and the consequent analysis of Compton-thick AGN with unprecedented sensitivity.

Table 2: Main characteristics of Lockman SpReSO

Parameter	Value
Centre coordinates	α:10h52m43s, δ:+57°28′48″
Spatial coverage	24×24 arcmin^2
Wavelength coverage	3500 – 9500Å
Spectral resolution	500–1000
Limiting continuum magnitude (3σ)	r′ AB 24.5
Total sources[a]	1171
FIR Herschel sources	952
Very red QSO[b]	72
Sub–mm galaxies [28]	30
Unstudied radio galaxies [8]	25
High proper motion Stars [39]	119
X-ray compact sources & CV candidates [14]	66
Ancillary data	Deep X-Ray through 6 cm

[a]Running out multiplicities
[b]Combining [18] and [35] criteria

4   Summary

OTELO is a unique survey in terms of minimum detectable flux and EW limit, that yields the deepest emission line survey to date with spectroscopic redshift accuracy. OTELO survey provides a database of emission line targets 20–50 times deeper than HiZELS [40] and with a density of emitter three times higher than those in COSMOS at an equivalent magnitude. The OTELO catalogue is scheduled to be public by the end of 2018. The main characteristics of the survey are summarized in Table 1.

Lockman SpReSO will constitute one of the deepest spectroscopic surveys of FIR-selected galaxies ever made: compared with other deep or ultra-deep spectroscopic surveys, Lockman SpReSO will reach a depth parameter [12] a factor 1.2 larger than the ongoing VVDS/ultra–deep survey [24]. Furthermore, this survey is more advantageous than

z-COSMOS and AEGIS–DEEP regarding the sensitivity at the continuum and the spectral coverage, respectively. Lockman SpReSO catalogue is tentatively scheduled to be public by 2020. The main characteristics of the survey are summarized in Table 2.

Acknowledgments

References

[1] Arnouts, S. et al. 1999, MNRAS 310, 540

[2] Barro, G. et al. 2011, ApJS 193, 30

[3] Bertin, E. Arnouts S. 1996, A&AS 317,393

[4] Bongiovanni, A. et al. 2016, in preparation

[5] Bongiovanni, A. et al. 2016, this volume

[6] Cepa, J. et al. 2008, A&A, 490, 1

[7] Cid–Fernandes, R. et al. 2010, MNRAS 403, 1036

[8] Ciliegi, M. et al., 2003, A&A, 398, 901

[9] Corral, A. et al.,2014, A&A, 569, 71

[10] Denicoló G., Terlevich R., Terlevich E. 2002, MNRAS 330, 69

[11] Dickey, J.M. and Lockman F.J. 1990, ARA&A 28, 215

[12] Djorgovski, S.G. et al., 2012, IAUS, 285, 141

[13] Domínguez-Sánchez, H. et al., 2014, MNRAS, 441, 2

[14] Drake, A.J. et al. 2014, MNRAS 441, 1186

[15] Fotopoulou, S. et al., 2012, ApJS, 198, 1

[16] Fujita, S.S. et al. 2003, ApJ, 586, 115

[17] Jones, D.H., Bland–Hawthorn, J., 2001, ApJ, 550, 593

[18] Glikman, E. et al. 2013, ApJ 778, 127

[19] González, J.J. et al. 2014, MNRAS 443, 3289

[20] Henry, J.P. et al., 2010, ApJ, 725, 615

[21] Huertas–Company, M. 2013, Astrophysics Source Code Library 1304.003

[22] Ilbert, O. et al. 2006, A&A 457, 841

[23] Kennicutt, R. et al., 1994, ApJ, 435, 22

[24] Le Févre, O. et al., 2013, A&A, 559, 14

[25] Lehmann, I. et al., 2001, A&A, 371, 833

[26] Lara–López, M.A. et al. 2011, PASP 123, 252

[27] Lutz, D. et al. 2011, A&A 532, 90

[28] Michalowski, M.J. et al. 2012, A&A 541, 85

[29] Nadolny, J. et al. 2016, this volume

[30] Newman, J.A. et al. 2013, ApJS 208, 5

[31] Oliver, S.J. et al. 2012, MNRAS 424, 1614

[32] Peng, C. et al. 2010, AJ 139, 2097

[33] Pović, M. et al. 2012, A&A 541, 118

[34] Ramón–Pérez, M. et al. 2016, this volume

[35] Ross, N.P. et al. 2015, MNRAS 453, 3932

[36] Rupke, D. et al., 2008, ApJ, 674, 192

[37] Sánchez–Portal, M. et al. 2015, A&A 578, 30

[38] Schmidt, M. et al., 1998, A&A, 329, 495

[39] Smart, R.L. and Nicastro, L. 2014, A&A 570, 87

[40] Sobral, D. et al 2013, MNRAS 428, 1128

[41] Stasinska, G., 2008, IAUS, 255, 375

[42] Steidel, C.C. et al., 2000, ApJ 532, 170

[43] Thommes, E. et al. 1997, Reviews in Modern Astronomy, 10, 297

[44] Zappacosta, L. et al., 2005, A&A, 434, 801